Multi-Components Interferometer Based on Partially Filled Dual-Core Photonic Crystal Fiber for Temperature and Strain Sensing

Maoxiang Hou, Ying Wang, Shuhui Liu, Zhihua Li, and Peixiang Lu

Abstract—A multi-components interferometer based on partially filled dual-core photonic crystal fiber (D-C PCF) was fabricated for measuring temperature and strain. The partially filled D-C PCF was prepared by manual gluing method, and the cladding air holes surrounding one core were selectively filled with refractive index liquid while remaining other air holes unfilled. A multi-components interference with a large spectrum envelope and fine interference fringes was observed in the transmission spectrum. Theoretical and experimental investigations revealed that the large spectrum envelope was originated from the interference between the fundamental modes of two cores of the PCF, while the fine interference fringes were generated by the interference between the fundamental mode and higher order modes in one core that surrounded by unfilled air holes. The proposed device can be used to monitor temperature and strain simultaneously through matrix demodulation, with a high temperature sensitivity of 5.43 nm/°C.

Index Terms—Optical fiber sensors, photonic crystal fibers, interferometer, dual-parameter sensor.

I. INTRODUCTION

PHOTONIC crystal fiber (PCF) is a type of microstructured optical fiber that contains solid cores surrounded by periodically arranged air holes in the fiber cladding, and is regarded as promising optical components due to its unique properties, such as high temperature stability, intrinsic micro-channels and flexibility of fiber design. Many kinds of sensors based on PCFs have been thoroughly investigated in monitoring various physical parameters including bending [1], strain [2], humidity [3], displacement [4], magnetic field [5], pressure [6], [7], refractive index (RI) [8] and temperature [9], etc. Nowadays, PCFs with selectively filled liquids have been a prominent research focus in the field of optical fiber sensing since the selectively infiltrated PCFs exhibited excellent properties of high spectral sensitivity [10]–[12], optical tunability [13] and flexible operation capability [14], [15].

In practical applications, the cross-sensitivity is a key issue since sensors are usually sensitive to more than one physical parameter, which will result in poor measurement precision. Recently, multi-parameter sensors have drawn great attention due to their capability of solving the cross-sensitivity between different parameters. Multi-parameter sensors usually consist of one or more sensing elements that have different responses to all measurands, which could be achieved by cascading several fiber devices [16], [17] or utilizing different optical modes in a single fiber structure [18]. Many techniques have been proposed to achieve multi-parameter sensing, such as dual-pass interferometers [19], [20], fiber gratings combined with PCFs [21], [22], multimode-fiber-based interferometers [23]–[25], and selectively infiltrated PCFs with wavelength- or mode-dependent sensitivities [26]–[28]. However, dual-pass interferometers require extra optical delay line and couplers, and multimode fiber based interferometers exhibit relatively low sensitivities. Meanwhile, fiber gratings and selectively infiltrated PCFs require exact and sophisticated operations, which enhanced the complexity of the device fabrication.

In this paper, we demonstrate a multi-components interferometer based on a partially liquid-filled dual-core (D-C) PCF for temperature and strain sensing. The D-C PCF was prepared by manual-gluing method, and air holes on one side of the two fiber cores were selectively filled with RI liquid and the others were not. The effective modal RI difference (Δn) between the two cores were greatly changed after the infiltration process. A large spectrum envelope with fine interference fringes can be observed in the transmission spectra of the multi-components interferometer. Modal analysis shows that the interference with large FSR was originated from the interference between the fundamental modes of two cores of the PCF while the fine interference fringes were generated by the interference between the fundamental mode and higher order modes in one core that surrounded by unfilled air holes.

M. Hou and Z. Li are with the Wuhan National Laboratory for Optoelectronics, School of Physics, Huazhong University of Science and Technology, Wuhan 430074, China (e-mail: d201277029@hust.edu.cn; lizhihua@mail.hust.edu.cn).

Y. Wang is with the College of Optoelectronic Engineering, Shenzhen University, Shenzhen 518060, China (e-mail: yingwang@szu.edu.cn).

S. Liu is with the Laboratory of Optical Information Technology, Wuhan Institute of Technology, Wuhan 430205, China (e-mail: lsh20060388@163.com).

P. Lu is with the Wuhan National Laboratory for Optoelectronics, School of Physics, Huazhong University of Science and Technology, Wuhan 430074, China, and also with the Laboratory of Optical Information Technology, Wuhan Institute of Technology, Wuhan 430205, China (e-mail: lupeixiang@mail.hust.edu.cn).
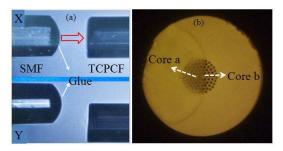
Fig. 1. (a) Microscopic image to explain the optical alignment and manual gluing procedure for the partially blocked process. The glue-dispensed fiber tip mounted on the V-groove of a fiber fusion splicer was moved and contacted the cleaved D-C PCF with a big offset. (b) The cross-section view of the partially blocked D-C PCF. The cladding air holes surrounding of core *a* were blocked by glue, while air holes surrounding of core *b* were remained.

The large spectrum envelope exhibited a temperature sensitivity of 5.43 nm/°C and a strain sensitivity of −1.95 pm/$\mu\varepsilon$, while those of the fine interference fringes were 0.012 nm/°C and −2.08 pm/$\mu\varepsilon$, respectively. By monitoring the wavelength shifts of both fringes simultaneously, the multi-components interferometer can be used as a dual-parameter sensor through matrix demodulation. Moreover, this proposed sensor exhibits the advantages of high sensitivity, low cost, and simplicity for manufacture, which make it a good candidate for multiple parameters simultaneously measurements.

II. STRUCTURE AND PRINCIPLES

The D-C PCF used in the experiments (YOFC Ltd.) has an outer cladding with a diameter of 125 μm and 5 rings of circular air holes hexagonal arranged in the cross-section of the cladding, and two solid cores located symmetrically on two sides of the fiber center. The diameter of the air holes is about 3 μm with a hole pitch Λ of 3.7 μm [29]. The manual gluing procedure for the partially blocking process was operated on a fusion splicer (Fujikura FSM-80S). Firstly, a cleaved single mode fiber (SMF) was dip coated with a drop of glue (502 superglue No.7146 from Deli Group Co., Ltd.) at the fiber end, and carefully positioned on a stepping motor of the fusion splicer. Then a cleaved D-C PCF was placed on the other stepping motor, and the two fibers were aligned in X-axis and offset greatly in Y-axis. Thereafter, the glue-dispensed SMF tip was moved towards the D-C PCF along the X-axis so that the glue on the SMF end can be transferred to the D-C PCF to block half of air holes at the end-facet, as shown in Fig. 1(a).

Fig. 1(b) shows the cross-section of the partially glue blocked D-C PCF, where the cladding air holes that surrounding one of the PCF fiber core *a* are blocked by glue. As the glue cured, the partially blocked D-C PCF was immersed into RI liquid that has a thermal-optic coefficient of −3.41 × 10⁻⁴RIU/°C (1.36±0.001, from Cargille Labs). The liquid was infiltrated into the unblocked air holes surrounding core *b* due to capillary force. After infiltration, the liquid-filled PCF was cleaved from the non-immersed fiber end and the glue blocked end to ensure the PCF to be used is filled with RI liquid. Then, the liquid-filled PCF was spliced between two sections of SMFs, and an offset is induced in one splicing joint to excite higher order modes [22], [28]. Noting that a fraction
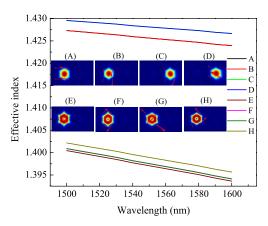

Fig. 2. Simulation of the first eight mode fields and their dispersion curves of the partially filled D-C PCF; inset: (A-B) the mode profiles of the LP$_{01}$ of core *a*, (C-D) the mode profiles of the LP$_{01}$ mode of core *b*, and (E-H) the mode profiles of the LP$_{11}$ mode of core *a*.

of RI liquid at the end of the PCF was vaporized by pre-arcing before splicing [21]. With this method, a multi-components interference was realised in the partially liquid filled D-C PCF and makes it possible to dual-parameter measurements. The purpose of partially liquid-infiltration is to break the two-fold symmetry of the D-C PCF, so that the temperature-dependence of effective modal RIs of core *b* can be significantly enhanced while those of core *a* are hardly affected.

The modal characteristics of the partially filled D-C PCF have been simulated by the full-vector finite element method, with material dispersions being considerate. Compared with the unfilled PCF, the modal properties have been tailored significantly. The mode field distributions and dispersion curves of the fundamental modes and the higher-order core modes were plotted in insets *A-G* of Fig. 2. Modes *A* and *B* are the fundamental modes of core *a* with perpendicular electric field directions, and modes *C* and *D* are the fundamental modes of core *b*. Modes *E-H* are a group of higher-order modes of core *a* with four different polarization directions. As can be seen from Fig. 2, modes *A* and *B* are degenerated modes and their dispersion curves are approximately overlapped, which are the same for modes *C* and *D*. The Δn between the fundamental modes of core *a* and core *b* was calculated to be 2.489 × 10⁻³, and the Δn between the fundamental mode and the four high order modes of core *a* at 1550 nm were 2.856 × 10⁻², 2.809 × 10⁻², 2.809 × 10⁻² and 2.67 × 10⁻², respectively.

The modal interference (MI) of the proposed sensor can be described by the following equation [30],

$$I = I_1 + I_2 + 2\sqrt{I_1 I_2} cos\varphi, \qquad (1)$$

where I_1 and I_2 are light intensities of two modes that involves in the interference. The free spectral range (FSR) is given by

$$FSR = \frac{\lambda^2}{\Delta n L}, \qquad (2)$$

where $\Delta n = n_1 - n_2$, n_1 and n_2 represent the effective RIs of the two modes, and L is the length of the interference arm. When ambient temperature changes, the RI of filled liquid changes significantly due to the thermal-optic effect, which will cause a phase change $\Delta\varphi$ of the
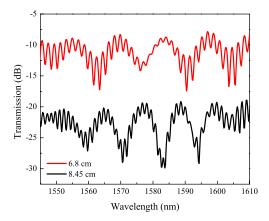
Fig. 3. Transmission spectra of the proposed multi-components interference sensors with different PCF lengths.

multi-components interferometer. The phase change induced by temperature can be described as [31]

$$\Delta\varphi = \frac{2\pi(\frac{\partial \Delta n}{\partial T}L + \frac{\partial L}{\partial T}\Delta n)\Delta T}{\lambda}. \tag{3}$$

Ignoring the thermal expansion effect, the shift of dip wavelength can be derived as [32]

$$\Delta\lambda_{dip} = -FSR(\frac{\Delta\varphi}{2\pi}) = -\lambda_0 \Delta T \frac{1}{\Delta n}\frac{\partial \Delta n}{\partial T}. \tag{4}$$

According to equation 4, a higher relative thermal coefficient $\partial \Delta n/\partial T$ may result in a higher temperature sensitivity.

Fig. 3 shows the transmission spectra of partially liquid filled D-C PCF based interferometers with lengths (L) of 8.45 and 6.80 cm, respectively. The spectra were measured by using an ASE light source (ALS-1550-20) and an optical spectrum analyzer (OSA, Yokogawa AQ6370B) with a resolution of 10 pm. As can be seen in Fig. 3, each transmission spectrum is consisted of two-components interference, i.e., a large spectrum envelope and a fine interference fringe. The relative large insertion loss of the device with PCF length of 6.80 cm is ~10 dB, which includes the splicing loss and the liquid filling loss. A shorter device will have a smaller loss. The *FSRs* of the large spectrum envelope and the fine interference for the sample with a PCF length of 8.45 cm around 1550 nm are 11.22 and 1.29 nm, respectively. While for the sample with a PCF length of 6.80 cm, the *FSR*s are 13.6 and 1.31 nm, respectively. By using equation (2), the Δn between the interference modes were calculated to be 2.534×10^{-3} and 2.204×10^{-2} for the former one, 2.598×10^{-3} and 2.697×10^{-2} for the latter, respectively. The slight difference of calculated Δn between the two samples may be due to measurement errors of the PCF lengths. Contrasted the simulated effective RI of each mode with the calculated Δn from the transmission spectra, we can conclude that the large spectrum envelope is originated from the interference between the fundamental modes of core *a* and core *b*, and the fine fringes are due to the interference between the fundamental mode and its higher order modes of core *a*.

The thermal-optic coefficients of the eight modes listed in Fig. 2 were simulated and shown in Fig. 4. According to the calculated thermal-optic coefficient and corresponding effective RI of each mode, the temperature sensitivities of
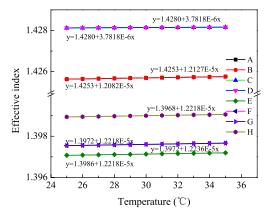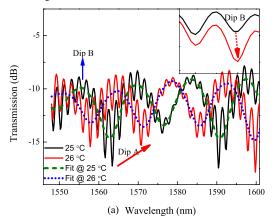

Fig. 4. Simulated thermal-optic coefficients of the modes shown in insets of Fig. 2, at wavelength of 1550 nm.
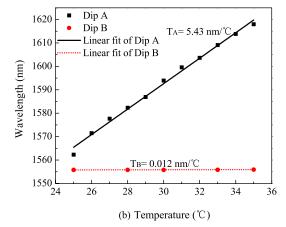

(a) Wavelength (nm)

(b) Temperature (℃)

Fig. 5. (a) Transmission spectra of the proposed multi-components interference sensor at 25°C and 26°C, with a PCF length of 6.8 cm, inset: magnified fringe of dip B in a small spectral range. (b) Wavelength shifts of dip A and dip B as a function of temperature.

the large spectrum envelope and the fine interference fringes around 1550 nm can be predicted to be 5.17 nm/°C and 0.008 nm/°C by using equation (4), respectively. According to Eq.(4), higher thermal coefficient may result in a higher temperature sensitivity, thus the RI liquid used here with high thermal-optic coefficients will cause the high sensitivity of the larger spectrum envelope.

III. EXPERIMENTAL RESULTS

The temperature response of the partially filled D-C PCF interferometer has been studied experimentally.
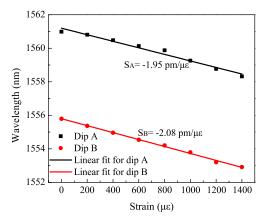
Fig. 6.   Wavelength shifts of dip A and dip B as a function of strain.

Temperature responses of the samples were tested in a column oven, where the samples are fixed straightly inside the oven to avoid any bending perturbations. Temperature in the oven increased gradually from 25°C to 35°C with a step of 1 °C, and then maintained about 5 min at each temperature point. As shown in Fig. 5(a), the olive dashed line and the blue dashed line were fitted of the large spectrum envelope at 25 °C and 26 °C, respectively, for the sample with a PCF length of 6.8 cm. As the temperature increased, dip A (one dip of the large spectrum envelope, as marked in Fig. 5(a)) exhibited a large red shift, while dip B (one dip of the fine interference fringes, also marked in Fig. 5(a)) showed a relatively small shift, as can be seen in the inset of Fig. 5(a). The wavelength shifts of dips A and B in a temperature range from 25°C to 35°C were shown in Fig. 5(b), where the temperature sensitivities are 5.43 nm/°C and 0.012 nm/°C for dip A and dip B, respectively.

The measured sensitivities of the sensor are consistent with the theoretical ones, which also verified that the large spectrum envelope is originated from the interference between the fundamental modes of core *a* and core *b*, and the fine fringes are due to the interference between the fundamental mode and higher order mode of core *a*. The small deviation between the measured and the calculated values is mainly come from the errors of the geometrical structure parameters of the PCF used in the theoretical calculations, as mentioned in [27]. The high temperature sensitivity of the large spectrum envelope is attributed to the high thermal-optic coefficient of the RI liquid which makes the effective RI of core mode in one core sensitive to ambient temperature while that in the other core insensitive. The sensitivity of the proposed sensor exhibit a significant improvement compared with the unfilled PCF-based Mach-Zehnder interferometer (MZI) device [29].

The strain sensing characteristics of the multi-components interferometer was also investigated with a strain test system. The experiment was carried out under a constant temperature of 25 °C to avoid temperature perturbations. The wavelength shifts of dips A and B were plotted in Fig. 6 with the applied strain ranging from 0 to 1400 $\mu\varepsilon$. Dips A and B exhibited strain sensitivities of -1.95 pm/$\mu\varepsilon$ and -2.08 pm/$\mu\varepsilon$, respectively, which are comparable to that of the previously reported D-C PCF-based MZI device [29].

The cross sensitivity of temperature and strain can be solved by using the standard matrix demodulation method [24], so simultaneous measurements of strain and temperature can be achieved with the proposed interferometer by calculating a sensitivity matrix as below

$$\begin{bmatrix} \Delta T \\ \Delta \varepsilon \end{bmatrix} = \begin{bmatrix} 5.43 \; nm/°C & -1.95 \; pm/\mu\varepsilon \\ 0.012 \; nm/°C & -2.08 \, pm/\mu\varepsilon \end{bmatrix}^{-1} \begin{bmatrix} \Delta\lambda_{dipA} \\ \Delta\lambda_{dipB} \end{bmatrix}.$$
(5)

In the matrix, ΔT and $\Delta\varepsilon$ are the temperature and strain variations, respectively, and $\Delta\lambda_{dipA}$ and $\Delta\lambda_{dipB}$ represent the wavelength shifts of dips A and B, respectively. With assuming a resolution of 10 pm of the OSA, the strain and temperature resolution can be estimated to be about $\pm 5\mu\varepsilon$ and ± 0.004°C, respectively, according to the method mentioned in Ref. [24].

IV. CONCLUSIONS

In summary, an interferometer based on partially liquid filled dual-core PCF was investigated for temperature and strain sensing. The transmission spectrum of the device contains two sets of interferences, a large spectrum envelope originated from the interference between the fundamental modes of two cores of the PCF, and fine interference fringes generated by the interference between the fundamental mode and higher order modes in one core that surrounded by unfilled air holes. This sensor exhibited a high temperature sensitivity of up to 5.43 nm/°C, which is benefit from the high thermal-optic coefficient of the selectively filled liquid in the dual-core PCF. The multi-components interferometer can be used as a dual-parameter sensor through matrix demodulation. The proposed sensor exhibits practical advantages such as high sensitivity, flexibility of fabrication and capability for dual parameter sensing, which may find potential applications in physical sensing and structural health monitoring.

REFERENCES

[1] S. Liu, N. Liu, M. Hou, J. Guo, Z. Li, and P. Lu, "Direction-independent fiber inclinometer based on simplified hollow core photonic crystal fiber," *Opt. Lett.*, vol. 38, no. 4, pp. 449–451, Feb. 2013.

[2] J. Villatoro, V. Finazzi, V. P. Minkovich, V. Pruneri, and G. Badenes, "Temperature-insensitive photonic crystal fiber interferometer for absolute strain sensing," *Appl. Phys. Lett.*, vol. 91, no. 9, p. 091109, Aug. 2007.

[3] J. Mathew, Y. Semenova, and G. Farrell, "Effect of coating thickness on the sensitivity of a humidity sensor based on an agarose coated photonic crystal fiber interferometer," *Opt. Exp.*, vol. 21, no. 5, pp. 6313–6320, Mar. 2013.

[4] J. N. Dash, R. Jha, J. Villatoro, and S. Dass, "Nano-displacement sensor based on photonic crystal fiber modal interferometer," *Opt. Lett.*, vol. 40, no. 4, pp. 467–470, Feb. 2015.

[5] R. Gao and Y. Jiang, "Magnetic fluid-filled microhole in the collapsed region of a photonic crystal fiber for the measurement of a magnetic field," *Opt. Lett.*, vol. 38, no. 16, pp. 3181–3184, Feb. 2013.

[6] Z. Liu, M.-L. V. Tse, C. Wu, D. Chen, C. Lu, and H.-Y. Tam, "Intermodal coupling of supermodes in a twin-core photonic crystal fiber and its application as a pressure sensor," *Opt. Exp.*, vol. 20, no. 19, pp. 21749–21757, Sep. 2012.

[7] M. Hou, Y. Wang, S. Liu, J. Guo, Z. Li, and P. Lu, "Sensitivity-enhanced pressure sensor with hollow-core photonic crystal fiber," *J. Lightw. Technol.*, vol. 32, no. 23, pp. 4637–4641, Dec. 1, 2014.

[8] Y. Wang, D. N. Wang, C. R. Liao, T. Hu, J. Guo, and H. Wei, "Temperature-insensitive refractive index sensing by use of micro Fabry–Pérot cavity based on simplified hollow-core photonic crystal fiber," *Opt. Lett.*, vol. 38, no. 3, pp. 269–271, Jun. 2013.

[9] Y. Li, W. Chen, H. Wang, N. Liu, and P. Lu, "Bragg gratings in all-solid Bragg photonic crystal fiber written with femtosecond pulses," *J. Lightw. Technol.*, vol. 29, no. 22, pp. 3367–3371, Nov. 15, 2011.

[10] Y. Wang, M. Yang, D. N. Wang, and C. R. Liao, "Selectively infiltrated photonic crystal fiber with ultrahigh temperature sensitivity," *IEEE Photon. Technol. Lett.*, vol. 23, no. 20, pp. 1520–1522, Oct. 15, 2011.

[11] M. Yang, D. N. Wang, Y. Wang, and C. R. Liao, "Fiber in-line Mach–Zehnder interferometer constructed by selective infiltration of two air holes in photonic crystal fiber," *Opt. Lett.*, vol. 36, no. 5, pp. 636–638, Mar. 2011.

[12] Y. Geng, X. Li, X. Tan, Y. Deng, and X. Hong, "Compact and ultra-sensitive temperature sensor with a fully liquid-filled photonic crystal fiber Mach–Zehnder interferometer," *IEEE Sensors J.*, vol. 14, no. 1, pp. 167–170, Jan. 2014.

[13] Y. Liu *et al.*, "Compact tunable multibandpass filters based on liquid-filled photonic crystal fibers," *Opt. Lett.*, vol. 39, no. 7, pp. 2148–2151, Apr. 2014.

[14] C. Yang *et al.*, "Selectively liquid-infiltrated microstructured optical fiber for simultaneous temperature and force measurement," *IEEE Photon. J.*, vol. 6, no. 2, Apr. 2014, Art. no. 6800808.

[15] K. Naeem, B. H. Kim, B. Kim, and Y. Chung, "High-sensitivity temperature sensor based on a selectively-polymer-filled two-core photonic crystal fiber in-line interferometer," *IEEE Sensors J.*, vol. 15, no. 7, pp. 3998–4003, Jul. 2015.

[16] M. M. Ali, R. Islam, K.-S. Lim, D. S. Gunawardena, H.-Z. Yang, and H. Ahmad, "PCF-cavity FBG Fabry–Perot resonator for simultaneous measurement of pressure and temperature," *IEEE Sensors J.*, vol. 15, no. 12, pp. 6921–6925, Dec. 2015.

[17] Q. Liu, Z. L. Ran, Y. J. Rao, S. C. Luo, H. Q. Yang, and Y. Huang, "Highly integrated FP/FBG sensor for simultaneous measurement of high temperature and strain," *IEEE Photon. Technol. Lett.*, vol. 26, no. 17, pp. 1715–1717, Sep. 1, 2014.

[18] W. Lin *et al.*, "Liquid-filled photonic-crystal-fiber-based multimodal interferometer for simultaneous measurement of temperature and force," *Appl. Opt.*, vol. 54, no. 6, pp. 1309–1313, Feb. 2015.

[19] H. Luo, Q. Sun, Z. Xu, D. Liu, and L. Zhang, "Simultaneous measurement of refractive index and temperature using multimode microfiber-based dual Mach–Zehnder interferometer," *Opt. Lett.*, vol. 39, no. 13, pp. 4049–4052, Jul. 2014.

[20] S. Wang, P. Lu, L. Mao, D. Liu, and S. Jiang, "Cascaded interferometers structure based on dual-pass Mach–Zehnder interferometer and Sagnac interferometer for dual-parameter sensing," *Opt. Exp.*, vol. 23, no. 2, pp. 674–680, Jan. 2015.

[21] G. Yin *et al.*, "Simultaneous refractive index and temperature measurement with LPFG and liquid-filled PCF," *IEEE Photon. Technol. Lett.*, vol. 27, no. 4, pp. 375–378, Feb. 15, 2015.

[22] W. Huang *et al.*, "Multi-component-intermodal-interference mechanism and characteristics of a long period grating assistant fluid-filled photonic crystal fiber interferometer," *Opt. Exp.*, vol. 22, no. 5, pp. 5883–5894, Mar. 2014.

[23] B. Dong, J. Hao, C. Y. Liaw, and Z. Xu, "Cladding-mode resonance in polarization-maintaining photonic-crystal-fiber-based Sagnac interferometer and its application for fiber sensor," *J. Lightw. Technol.*, vol. 29, no. 12, pp. 1759–1763, Jun. 15, 2011.

[24] C. Chen *et al.*, "Compact fiber tip modal interferometer for high-temperature and transverse load measurements," *Opt. Lett.*, vol. 38, no. 17, pp. 3202–3204, Sep. 2013.

[25] S. Rota-Rodrigo, M. López-Amo, J. Kobelke, K. Schuster, J. L. Santos, and O. Frazão, "Multimodal interferometer based on a suspended core fiber for simultaneous measurement of physical parameters," *J. Lightw. Technol.*, vol. 33, no. 12, pp. 2468–2473, Jun. 15, 2015.

[26] H. Liang *et al.*, "Simultaneous measurement of temperature and force with high sensitivities based on filling different index liquids into photonic crystal fiber," *Opt. Lett.*, vol. 38, no. 7, pp. 1071–1073, Apr. 2013.

[27] H. Liang *et al.*, "Fiber in-line Mach–Zehnder interferometer based on near-elliptical core photonic crystal fiber for temperature and strain sensing," *Opt. Lett.*, vol. 38, no. 20, pp. 4019–4022, Oct. 2013.

[28] M. Luo, Y.-G. Liu, Z. Wang, T. Han, J. Guo, and W. Huang, "Microfluidic assistant beat-frequency interferometer based on a single-hole-infiltrated dual-mode microstructured optical fiber," *Opt. Exp.*, vol. 22, no. 21, pp. 25224–25232, Oct. 2014.

[29] S. Liu, N. Liu, Y. Wang, J. Guo, Z. Li, and P. Lu, "Simple in-line M–Z interferometer based on dual-core photonic crystal fiber," *IEEE Photon. Technol. Lett.*, vol. 24, no. 19, pp. 1768–1770, Oct. 1, 2012.

[30] W. S. Mohammed, A. Mehta, and E. G. Johnson, "Wavelength tunable fiber lens based on multimode interference," *J. Lightw. Technol.*, vol. 22, no. 2, pp. 469–477, Feb. 2004.

[31] W. Qian *et al.*, "Temperature sensing based on ethanol-filled photonic crystal fiber modal interferometer," *IEEE Sensors J.*, vol. 12, no. 8, pp. 2593–2597, Aug. 2012.

[32] G. Coviello, V. Finazzi, J. Villatoro, and V. Pruneri, "Thermally stabilized PCF-based sensor for temperature measurements up to 1000 °C," *Opt. Exp.*, vol. 17, no. 24, pp. 21551–21559, Nov. 2009.

Maoxiang Hou received the B.Sc. degree in applied physics from Northeastern University, Shenyang, China, in 2011. He is currently pursuing the Ph.D. degree with the School of Physics, Huazhong University of Science and Technology, Wuhan, China.

Ying Wang received the B.Sc. degree in applied physics and the Ph.D. degree in physical electronics from the Huazhong University of Science and Technology, Wuhan, China, in 2004 and 2010, respectively. He was with the College of Optoelectronic Engineering, Shenzhen University, as a Lecturer, in 2015. His research interests are optical fiber sensors and femtosecond laser micromachining.

Shuhui Liu received the B.Sc. degree in electronic science and technology from the Beijing Institute of Technology, Beijing, China, in 2010, and the Ph.D. degree from the School of Optical and Electronic Information, Huazhong University of Science and Technology, Wuhan, China, in 2015. He was with the School of Science, Wuhan Institute of Technology, as a Lecturer, in 2015.

Zhihua Li received the B.Sc. degree in physics from Wuhan University, and the master's and Ph.D. degrees in physics from the Huazhong University of Science and Technology, Wuhan, China, in 1998, 2001, and 2004, respectively. She was with the School of Physics, Huazhong University of Science and Technology, as a Professor, in 2014. Her main research interests include theoretical and experimental research for interaction of femtosecond laser and materials.

Peixiang Lu received the B.Sc. degree in physics from Beijing University, Beijing, China, in 1987, and the Ph.D. degree from the Shanghai Institute of Optics and Fine Mechanics, Chinese Academy of Sciences, Beijing, in 1992. He is currently a Professor with the School of Physics and Wuhan National Laboratory for Optoelectronics, Huazhong University of Science and Technology, Wuhan, China. His main research interests include ultrafast optics, femtosecond laser micromachining, and fiber laser.